Nanotechnology

DOI: 10.1002/anie.201000659

Carbon Nanotubes with Titanium Nitride as a Low-Cost Counter-Electrode Material for Dye-Sensitized Solar Cells**

Guo-ran Li, Feng Wang, Qi-wei Jiang, Xue-ping Gao, and Pan-wen Shen*

Dye-sensitized solar cells (DSSCs) are promising candidates for low-cost and clean energy conversion devices.[1–4] In the development of DSSCs, key challenges include the demonstration of high efficiency and scale-up of fabrication.[3] As the conventional counter-electrode material in the devices, platinum, is a burden for large-scale applications of DSSCs because it is one of the most expensive materials available.[3,5] Furthermore, the sustaining improvement of semiconductor electrode and electrolyte poses higher demand on counter-electrode performance.[5,6] Therefore, it is necessary to develop low-cost and platinum-free counter-electrode materials with relatively high conversion efficiency for DSSCs.

The counter electrode in DSSCs promotes the electron translocation from the external circuit back to the redox electrolyte, and catalyzes the reduction of triiodide ions. Therefore, counter-electrode materials of high electrical conductivity and superior electrocatalytic activity are highly desired.[5,7] However, it is usually not easy to meet the both above requirements simultaneously. Generally, small particles provide high electrocatalytic activity owing to the large surface area, but they also lower electron transport efficiency owing to the abundant grain boundaries and defects.[8] According to previous studies, carbonaceous materials, such as carbon nanotubes (CNTs),[9,10] carbon black,[11] mesoporous carbon,[12] activated carbon,[13] fullerene,[14] and electroconductive polymers,[14,15] generally show good performance because the large surface area of the materials can redress the low intrinsic electrocatalytic activity of carbon. Grätzel and co-workers recently deposited electrochemically CoS nanoparticles on PEN/ITO film with good electrical conductivity to obtain a high-performance platinum-free counter electrode with a remarkable cell stability.[16]

To combine both high electrical conductivity and superior electrocatalytic activity in one material, we propose an alternative design for the fabrication of low-cost and platinum-free counter-electrode materials by constructing a fast electron-transport network and creating highly active sites on the electron pathway. Multi-walled carbon nanotubes can be considered as a fast electron-transport network because of the coexistence of ballistic and diffusive transport[17] and the tubular morphology.[10] Furthermore, CNTs possess electrocatalytic activity for the reduction of triiodide ions to a certain extent,[9–10] and their good mechanical properties are also helpful for the formation of electrode film.[18] Therefore, CNTs are suitable matrix material for constructing a fast electron-transport network. Regarding the highly efficient electrocatalyst, titanium nitrides (TiN) demonstrate high intrinsic electrocatalytic activity for the reduction of triiodide ions owing to the similarity of the electronic structure of the metal nitrides to that of the noble metals.[19,20] A DSSC composed of the highly ordered TiN nanotube arrays shows comparable performance with typical Pt counter electrode.[20] However, TiN nanoparticle film electrode alone has lower fill factor (*FF*) owing to the poor electron transport efficiency across nanoparticles.[20] Furthermore, the introduction of conducting paths of CNTs into TiN can improve electrical conductivity and capacitance of TiN.[21] Herein, we demonstrate that low-cost TiN-CNTs, fabricated by anchoring TiN nanoparticles on the CNTs network, can provide simultaneous high electrical conductivity and superior electrocatalytic activity.

TiN-CNTs were prepared by thermal hydrolysis of $TiOSO_4$ on CNTs and subsequent nitridation in an ammonia atmosphere. XRD results indicate that the as-prepared sample consists of cubic TiN (JCPDS 87-0633) and carbon nanotubes. No peaks of other titanium species are observed in the XRD pattern (Supporting Information, Figure S1). Structural details of TiN-CNTs were investigated using TEM and STEM with EDS. TiN nanoparticles, with a size of less than 10 nm, are dispersedly loaded on the surface of CNTs (Figure 1 a), whilst no TiN aggregates are observed because of the slow hydrolysis of $TiOSO_4$, with a low concentration under the moderate conditions.[22] A HRTEM image (Figure 1 b) confirms that TiN nanoparticles have a relatively high crystallinity and an average size of 5–10 nm. Furthermore, the walls of CNTs are locally distorted near TiN nanoparticles, indicating a strong interaction between TiN nanoparticles and CNTs, which possibly originates from the hydrolysis reaction between hydroxy groups on CNTs and the titanium salt[23] used in the preparation process. The strong interaction causes the TiN nanoparticles to be tightly loaded on CNTs, and electron transport between TiN and CNTs occurs easily. The element distribution of TiN-CNTs is investigated by EDS line-scanning. In the STEM image (Figure 1 c), TiN nanoparticles show a white contrast owing to the high atomic number of titanium compared to carbon.[24] EDS line-scanning, taken across a single carbon nanotube in Figure 1 c from right to left, is shown in Figure 1 d. Qualitatively, a

[*] Dr. G. R. Li, F. Wang, Dr. Q. W. Jiang, Prof. X. P. Gao, Prof. P. W. Shen
Institute of New Energy Material Chemistry
Tianjin Key Laboratory of Metal- and
Molecule-Based Material Chemistry
Nankai University, Tianjin 300071 (China)
Fax: (+86) 22-2350-0876
E-mail: xpgao@nankai.edu.cn

[**] Financial Supports from the 973 Program (2009CB220100) of China is greatly appreciated.

Supporting information for this article is available on the WWW under http://dx.doi.org/10.1002/anie.201000659.

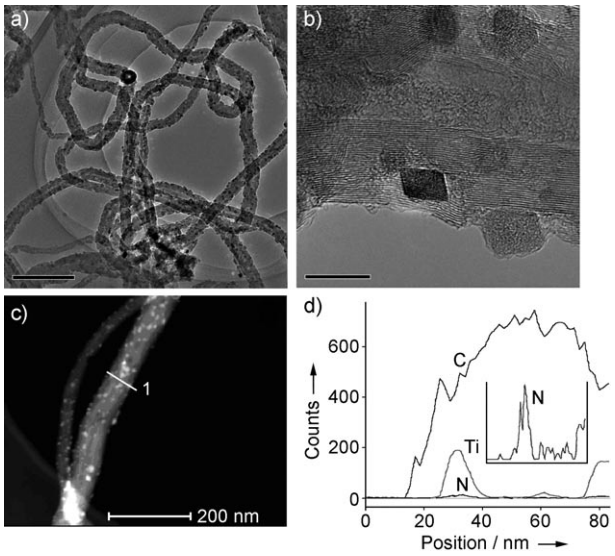

Figure 1. a,b) TEM images (scale bars: 200 nm (a), 10 nm (b)). c) HAADF-STEM image. d) Element distribution of TiN-CNTs. Inset: spectrum of N from 0 to 80 nm expanded vertically by a factor of 57.5. The signals in (d) were obtained by line-scanning across a single carbon nanotube (line **1** in (c)) from right to left.

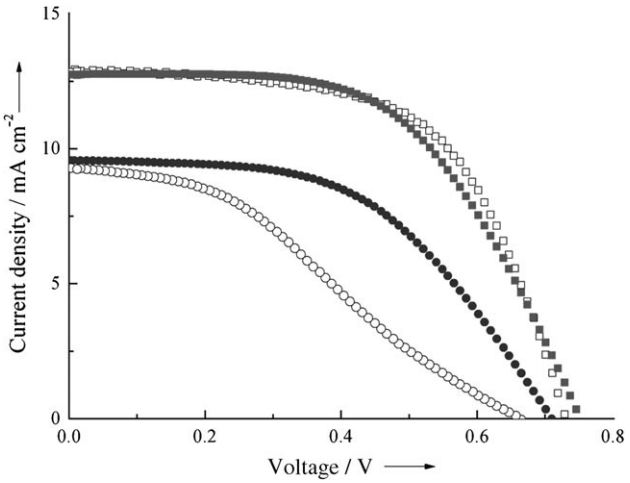

Figure 2. Characteristic *J–V* curves of DSSCs with different counter electrodes: TiN-CNTs (■, thickness 11.6 μm), CNTs (●, 11.0 μm), TiN nanoparticles (○, 11.2 μm), and Pt (□, 37 nm), measured under simulated sunlight 100 mW cm^{-2} (AM 1.5). The amount of active material is 0.63 mg per electrode (except for the Pt electrode).

Table 1: Photovoltaic parameters of DSSCs with different counter electrodes and the simulated data from EIS spectra.[a]

Sample	J_{sc} [mA cm^{-2}]	V_{oc} [V]	*FF*	η [%]	R_{ct} [Ω]	Z_w [Ω]	R_s [Ω]
TiN NPs	9.28	0.660	0.35	2.12	12.3	180.5	44.7
CNTs	9.55	0.705	0.52	3.53	37.5	40.2	33.5
TiN-CNTs	12.74	0.750	0.57	5.41	11.7	17.6	33.1
Pt	12.83	0.735	0.60	5.68	7.8	11.1	37.0

[a] For spectra, see Figure 3. V_{oc}: open-circuit voltage; J_{sc}: short-circuit current density; *FF*: fill factor; η: energy conversion efficiency. R_{ct}: charge-transfer resistance; Z_w: diffusion impedance; R_s: ohmic internal resistance.

strong peak intensity indicates the high element concentration at the corresponding location.[24] It is clear that the peak intensity of titanium and nitrogen increases simultaneously and that of carbon decreases in the white contrast area, further confirming the existence and high dispersion of TiN nanoparticles on CNTs. The results adequately describe the conformation of the as-prepared TiN-CNTs in which the active nanoparticles with a small size are dispersedly supported on CNT networks, as anticipated. The sample contains 10.0 wt% of titanium as detected by SEM-EDS (Supporting Information, Figure S2 and Table S1), and has a higher surface area (61.4 m^2 g^{-1}) than CNTs (56.7 m^2 g^{-1}).

Figure 2 shows *J–V* curves of the DSSCs using TiN-CNTs, CNTs, TiN nanoparticles, and Pt as counter electrodes. The detailed photovoltaic parameters from the *J–V* curves are summarized in Table 1. When the as-prepared TiN-CNTs are used as counter electrodes, the photovoltaic parameters are $V_{oc} = 0.750$ V, $J_{sc} = 12.74$ mA cm^{-2}, $FF = 0.57$, and $\eta = 5.41\%$. Obviously, all the photovoltaic parameters are higher than those of the DSSCs using CNTs and TiN nanoparticles, thus highlighting the predominant synergic effect of CNTs and TiN nanoparticles. The performance of the TiN-CNT counter electrode is generally comparable with that of the typical Pt counter electrode. Furthermore, the TiN-CNTs shows a slight advantage in open-circuit voltage owing to more interfacial active sites,[25] whilst the corresponding short-circuit current density and fill factor are little lower than those of Pt electrode. Therefore, the TiN-CNTs, fabricated by anchoring TiN nanoparticles on CNTs networks, may be a promising alternative to the conventional Pt electrode in DSSCs.

The effect of counter electrode on DSSC performance is mainly derived from different electrical conductivity and electrocatalytic activity for the reduction of triiodide to iodide.[5,7] In the cyclic voltammograms (CVs; Supporting Information, Figure S4), the peak positions of the TiN-CNTs are very similar to those of the Pt electrode, thus showing that TiN-CNTs have a similar electrocatalytic function to the Pt electrode. Furthermore, TiN-CNTs have a higher current density, suggesting a larger active surface.[16,26] However, the reduction reaction of triiodide ions on the CNTs is obviously slower. Thus, the introduction of TiN leads to an obvious improvement in the electrocatalytic activity. Figure 3 shows Nyquist plots of the symmetric configurations made by TiN-CNTs, CNTs, TiN nanoparticles, and Pt electrodes. The semicircle in the high frequency region corresponds to the charge-transfer process of electrolyte/electrode interface.[27] The charge-transfer resistance R_{ct} in the TiN-CNT and TiN nanoparticles is 11.7 Ω and 12.3 Ω, respectively. These values are close to that of the Pt electrode, indicating that TiN nanoparticles have a superior electrocatalytic activity. The semicircle in the low-frequency region is assigned to the Nernst diffusion process of triiodide ions.[10–11,28] TiN nanoparticles show a larger diffusion impedance (180.5 Ω) owing to low surface area (10.9 m^2 g^{-1}). The diffusion impedance of the TiN-CNTs is 17.6 Ω, which is much lower than the CNTs, and means that triiodide ions can be rapidly reduced to iodide ions under catalysis of TiN nanoparticles to accelerate diffusion of triiodide ions. Consequently, the overall impe-

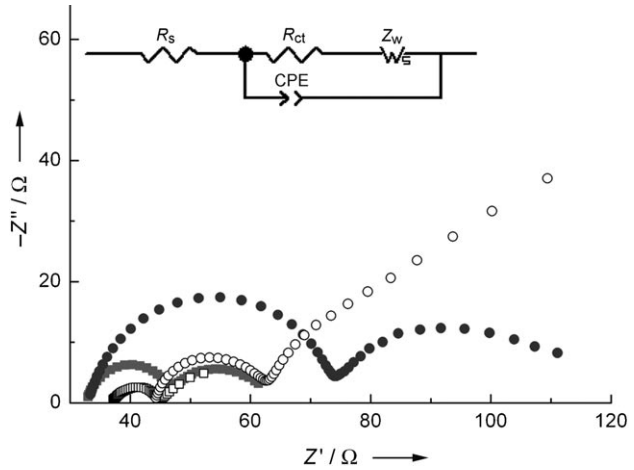

Figure 3. Equivalent circuit and Nyquist plots of the symmetric cells with two identical counter electrodes of TiN-CNTs (■), CNTs (●), TiN nanoparticles (○), or Pt (□). The cells were measured with the frequency range 100 kHz–100 mHz. R_{ct}: charge-transfer resistance, Z_w: diffusion impedance, R_s: ohmic internal resistance, CPE: constant phase element.

dance of the TiN-CNTs is very close to that of Pt electrode, resulting in the comparable photovoltaic performance.

As mentioned above, the combination of superior electrocatalytic activity and high electrical conductivity is an ideal strategy for developing highly efficient counter-electrode materials for DSSCs. In the TiN-CNTs, the superior electrocatalytic activity of TiN nanoparticles is undoubtedly the driving force for the high photovoltaic performance. Moreover, the introduction of TiN nanoparticles on CNTs not only decreases the charge-transfer resistance in the electrolyte/electrode interface, but also reduces the diffusion impedance of triiodide ions, leading to the high J_{sc} and *FF* for DSSCs. Meanwhile, the electron-transport network formed by CNTs also plays an indispensable role in the high photovoltaic performance. As shown in Figure 2, pure TiN nanoparticles without a CNTs network exhibit a very low *FF* and a poor photovoltaic performance because of the low surface area and the formation of a barrier to electron transport trapped at grain boundaries of TiN nanoparticles, demonstrating the importance of CNTs electron transport network. In fact, based on the same principle, CNTs supported Pt nanoparticles can be used as a counter electrode to obtain high photovoltaic performance (Supporting Information, Figure S6). Furthermore, the raw materials of the TiN-CNTs are inexpensive compared with the noble metal Pt, and the preparation process has low energy consumption, which makes TiN-CNTs cost-efficient and commercially viable.

In summary, TiN-CNTs were fabricated by hydrolysis of a titanium salt on CNTs and subsequent nitridation, in which TiN nanoparticles with a size of 5–10 nm are stably dispersed on the surface of CNTs. As a novel and low-cost counter-electrode material for DSSCs, TiN-CNTs show a comparable photovoltaic performance with the conventional Pt electrode, which is attributed to the ideal combination of superior electrocatalytic activity and high electrical conductivity derived from the unique structure, namely highly active TiN nanoparticles supported by a CNT electron-transport network. Such a design strategy is promising for fabricating highly efficient and low-cost counter-electrode materials for DSSCs.

Experimental Section

Preparation of TiN-CNTs: Commercial CNTs (Shenzhen NTP) were hydrothermally treated in NaOH aqueous solution (2 mol L^{-1}) for 2 h. The treated CNTs (0.5 g) were dispersed into $TiOSO_4$ aqueous solution (5 mL, 0.80 mol L^{-1}), and the resulting suspension was diluted with water to 500 mL and kept for 12 h at 80 °C. The solid product was recovered and rinsed with distilled water and then ethanol. After dried at 80 °C, the solid was calcined in a tubular furnace for 1 h at 800 °C in an ammonia atmosphere with a flow rate of 100 sccm to obtain TiN-CNTs.

Assembly of DSSCs: After soaking in ethanol, the TiN-CNTs powder was mixed with 1 % carboxymethyl cellulose (CMC) solution and stirred until a fluid mixture formed. A film was then made by the doctor-blade method on a FTO (fluorine-doped tin oxide) conductive glass (LOF, TEC-15, 15 Ω/square). The film was dried at 60 °C for 24 h to obtain TiN-CNTs counter electrodes. For comparison, a TiN blank CNT electrode was prepared by the same method, and a mirror-like Pt/FTO electrode was obtained by electrodepositing a platinum layer on the surface of FTO. A commercial TiO_2 sol (Solaronix, Ti-Nanoxide T/SP) was used to prepare TiO_2 film on FTO by the doctor-blade method, and the film was soaked in an ethanol solution of N-719 dye for 24 h to obtain dye-sensitized TiO_2 electrodes. Dye-sensitized solar cells were assembled by injecting the electrolyte into the aperture between the dye-sensitized TiO_2 electrode and the counter electrode. The liquid electrolyte composed of 0.05 M I_2, 0.1 M LiI, 0.6 M 1,2-dimethyl-3-propylimidazolium iodide (DMPII), and 0.5 M 4-*tert*-butyl pyridine with acetonitrile as the solvent. Surlyn 1702 was used as the spacer between the two electrodes. The two electrodes were clipped together and solid paraffin was used as sealant to prevent the electrolyte solution from leaking. The effective cell area was 0.25 cm^2.

X-ray diffraction (XRD) was performed on a Rigaku D/MAX-2500 diffractometer. Transmission electron microscopy (TEM) and scanning transmission electron microscopy (STEM) were performed on a FEI Tecnai F20 equipped with a high-angle annular dark field (HAADF) detector and an energy-dispersive X-ray spectrometer (EDS). Scanning electron microscopy (SEM) and SEM-EDS was performed on a Hitachi 4800 instrument. The DSSCs were illuminated by a solar simulator (CHF-XM500, Beijing Trusttech) under 100 mW cm^{-2} irradiation and calibrated by a standard silicon solar cell. Both the photocurrent-voltage (*J–V*) characteristic curves of the DSSCs under simulated sunlight and the electrochemical impedance spectroscopy (EIS) of the counter electrodes were recorded using an IM6ex (Zahner) electrochemical workstation. EIS spectra were measured in a symmetric cell configuration with two identical counter electrodes. The frequency range was from 100 kHz to 100 mHz with an AC modulation signal of 10 mV and bias DC voltage of 0.60 V.

Received: February 3, 2010
Published online: April 13, 2010

Keywords: carbon nanotubes · dyes/pigments · electrocatalysis · solar cells · titanium nitride

[1] B. O'Regan, M. Grätzel, *Nature* **1991**, *353*, 737.
[2] N. Armaroli, V. Balzani, *Angew. Chem.* **2007**, *119*, 52; *Angew. Chem. Int. Ed.* **2007**, *46*, 52.
[3] L. M. Peter, *Phys. Chem. Chem. Phys.* **2007**, *9*, 2630.

[4] T. W. Hamann, R. A. Jensen, A. B. F. Martinson, H. V. Ryswykac, J. T. Hupp, *Energy Environ. Sci.* **2008**, *1*, 66.
[5] N. Papageorgiou, *Coord. Chem. Rev.* **2004**, *248*, 1421.
[6] J. F. Qian, P. Liu, Y. Xiao, Y. Jiang, Y. L. Cao, X. P. Ai, H. X. Yang, *Adv. Mater.* **2009**, *21*, 3633.
[7] J. Halme, M. Toivola, A. Tolvanen, P. Lund, *Sol. Energy Mater. Sol. Cells* **2006**, *90*, 872.
[8] a) A. T. Bell, *Science* **2003**, *299*, 5613; b) S. H. Kang, S. H. Choi, M. S. Kang, J. Y. Kim, H. S. Kim, T. Hyeon, Y. E. Sung, *Adv. Mater.* **2008**, *20*, 54.
[9] a) H. W. Zhu, H. F. Zeng, V. Subramanian, C. Masarapu, K. H. Hung, B. Q. Wei, *Nanotechnology* **2008**, *19*, 465204; b) K. Suzuki, M. Yamaguchi, M. Kumagai, S. Yanagida, *Chem. Lett.* **2003**, *32*, 28; c) W. J. Lee, E. Ramasamy, D. Y. Lee, J. S. Song, *ACS Appl. Mater. Interfaces* **2009**, *1*, 1145.
[10] E. Ramasamy, W. J. Lee, D. Y. Lee, J. S. Song, *Electrochem. Commun.* **2008**, *10*, 1087.
[11] a) A. Kay, M. Grätzel, *Sol. Energy Mater. Sol. Cells* **1996**, *44*, 99; b) E. Ramasamy, W. J. Lee, D. Y. Lee, J. S. Song, *Appl. Phys. Lett.* **2007**, *90*, 173103.
[12] G. Q. Wang, W. Xing, S. P. Zhuo, *J. Power Sources* **2009**, *194*, 568.
[13] J. K. Chen, K. X. Li, Y. H. Luo, X. Z. Guo, D. M. Li, M. H. Deng, S. Q. Huang, Q. B. Meng, *Carbon* **2009**, *47*, 2704.
[14] T. Hino, Y. Ogawa, N. Kuramoto, *Carbon* **2006**, *44*, 880.
[15] a) Y. Saito, T. Kitamura, Y. Wada, S. Yanagida, *Chem. Lett.* **2002**, 1060; b) Z. P. Li, B. X. Ye, X. D. Hu, X. Y. Ma, X. P. Zhang, Y. Q. Deng, *Electrochem. Commun.* **2009**, *11*, 1768; c) J. G. Chen, H. Y. Wei, K. C. Ho, *Sol. Energy Mater. Sol. Cells* **2007**, *91*, 1472; d) J. B. Xia, N. Masaki, K. J. Jiang, S. Yanagida, *J. Mater. Chem.* **2007**, *17*, 2845; e) J. H. Wu, Q. H. Li, L. Q. Fan, Z. Lan, P. J. Li, J. M. Lin, S. C. Hao, *J. Power Sources* **2008**, *181*, 172.
[16] M. K. Wang, A. M. Anghel, B. Marsan, N. C. Ha, N. Pootrakulchote, S. M. Zakeeruddin, M. Grätzel, *J. Am. Chem. Soc.* **2009**, *131*, 15976.
[17] a) T. Umeyama, H. Imahori, *Energy Environ. Sci.* **2008**, *1*, 120; b) K. Ahmad, W. Pan, *Compos. Sci. Technol.* **2009**, *69*, 1016.
[18] E. T. Thostenson, T. W. Chou, *Adv. Mater.* **2006**, *18*, 2837.
[19] E. Furimsky, *Appl. Catal. A* **2003**, *240*, 1.
[20] Q. W. Jiang, G. R. Li, X. P. Gao, *Chem. Commun.* **2009**, 6720.
[21] L. Q. Jiang, L. Gao, *J. Am. Ceram. Soc.* **2006**, *89*, 156.
[22] J. P. Jolivet, *Metal Oxide Chemistry and Synthesis: From Solution to Solid State*, Wiley, New York, **2000**.
[23] D. Yang, G. Q. Guo, J. H. Hu, C. Wang, D. L. Jiang, *J. Mater. Chem.* **2008**, *18*, 350.
[24] X. W. Wang, X. P. Gao, G. R. Li, T. Y. Yan, H. Y. Zhu, *J. Phys. Chem. C* **2008**, *112*, 5384.
[25] B. A. Gregg, *Coord. Chem. Rev.* **2004**, *248*, 1215.
[26] Z. Huang, X. Z. Liu, K. X. Li, D. M. Li, Y. H. Luo, H. Li, W. B. Song, L. Q. Chen, Q. B. Meng, *Electrochem. Commun.* **2007**, *9*, 596.
[27] F. Fabregat-Santiago, J. Bisquert, E. Palomares, L. Otero, D. B. Kuang, S. M. Zakeeruddin, M. Grätzel, *J. Phys. Chem. C* **2007**, *111*, 6550.
[28] a) S. Sakurai, H. Q. Jiang, M. Takahashi, K. Kobayashi, *Electrochim. Acta* **2009**, *54*, 5463; b) L. Y. Han, N. Koide, Y. Chiba, A. Islam, R. Komiya, N. Fuke, A. Fukui, R. Yamanaka, *Appl. Phys. Lett.* **2005**, *86*, 213501.

